Supporting Information for

Synergistic force of green-synthesized zero-valent iron nanocomposites combined with different fertilizers for inhibiting cadmium accumulation in wheat

Lei Peng [a,c#], Yinglin Liu [a#], Nan Xu [a,b*], Yifei Feng [a,c], Jilong Xiong [a], Xuelian Wang [a], Wenxin Jiang [a], Jin Jin [c]

[a] School of Environmental Science and Engineering, Suzhou University of Science and Technology, Suzhou 215009, China

[b] Jiangsu Key Laboratory of Environmental Functional Materials, Suzhou University of Science and Technology, Suzhou 215009, China

[c] School of Chemistry and Life Sciences, Suzhou University of Science and Technology, Suzhou 215009, China

[#] Contribution equally

*Corresponding Authors: E-mail: nanxu@mail.usts.edu.cn

20 Pages; 1 Table and 6 Figures

SUPPLEMENTAL METHODS

Experiment S1: Characterization of GnZVI@DE.

Scanning electron microscopy (SEM; FEI Quanta 400 FEG, USA), X–ray diffraction (XRD; D8–Focus, Bruker AXS Co., Ltd., Germany), Fourier-transform infra-red spectrometer (FTIR, Nicolet iS10, Thermo Fisher Scientific, USA) and X–ray photoelectron spectroscopy (XPS, ESCALAB 250 XI, Thermo Fisher Scientific, USA) were used to characterize GnZVI@DE nanoparticles.

The SEM image of GnZVI@DE was shown in Figure S1A, it revealed the columnar structure of DE, and showed the porous structure of DE in its columnar cross section.[1] nZVI were unevenly dispersed on the porous cross section of DE, which was similar with other clay supported nZVI.

Additionally, GnZVI@DE was analyzed by XRD in Figure S1B.The XRD pattern of GnZVI@DE material showed that an inconspicuous peak at 2θ of 44.8° was characterized as Fe(0).[2, 3] The low resolution of the XRD peak indicated the Fe(0) core wrapped by excessive tea polyphenols coverage, which was in agreement with amorphous morphology of the synthesized materials reported by our previous study.[4] Another two obvious peaks at 2θ = 21.8° and 35.9° were identified as SiO_2 resulting from diatomite(DE) as main component.[1]

The XPS full scan spectrum was used to analysis the elementary composition of GnZVI@DE. As shown in Figure S1C, the appearance of obvious peaks for O 1s, C 1s, Fe 2p, N 1s and P 2p, and spectra confirmed that GnZVI@DE was successfully synthesized via the reaction of green tea extracts and Fe ions. Furthermore, IR peaks were analyzed to revel the surface functional groups of GnZVI@DE, which was elaborated in discussions about Figure 2A in main text.

Experiment S2: Plant Material and Growth Conditions

Wheat seeds were sterilized with 1%(v/v) sodium hypochlorite for 30 min, soaked in clean deionized (DI) water for 24 h (35℃, darkly). and then germinated on breeding trays in a growth

chamber (GXZ–280C, Ningbo Jiangnan Instrument Factory, China) with a 16h–light (at 25℃, 14400 Lux)/8h–dark (at 21℃, 0 Lux). After 1 weeks, seedlings were cultivated with modified full–strength Hoagland's nutrient solution (pH=6.0) in same growth chamber for 1 weeks.[5] As reported, Full–strength Hoagland's nutrient solution was containing with 4 mM $Ca(NO_3)_2 \cdot 4H_2O$, 6 mM KNO_3, 1 mM $NH_4H_2PO_4$, 2 mM $MgSO_4 \cdot 7H_2O$, 10 μM H_3BO_3, 1.8 μM $MnSO_4$, 0.2 μM $NaMoO_4$, 0.31 μM $CuSO_4$, 5 μM $ZnSO_4$, 50 μM Fe–EDDHA and 1mM KCl, pH=6.0). To investigate the Cd accumulation and translocation in wheat grown in Cd–contaminated soil/medium amended by GnZVI@DE in the presence of different nutrients, six nutrient combination solutions modified nutrient solution treatments were established as follows, NsA: NO_3^-–N & NH_4^+–N (14 mM & 1 mM), NsB: P (1 mM), NsC: NO_3^-–N & P (14 mM & 1 mM), NsD: NH_4^+–N & P (1 mM & 1 mM), NsE: NO_3^-–N & NH_4^+–N & P (14 mM & 1 mM & 1 mM) and NsF: urea–N & P (7.5 mM & 1 mM). To maintain the balance of calcium (Ca) and potassium (K), for the NsA, 1 mM $NH_4H_2PO_4$ were replaced with 1 mM NH_4Cl. For the NsB, 4 mM $Ca(NO_3)_2 \cdot 4H_2O$, 6 mM KNO_3 and 1 mM $NH_4H_2PO_4$ were replaced with 4 mM $CaCl_2$, 6 mM KCl and 1 mM KH_2PO_4, respectively. For the NsC, 1 mM KCl and 1 mM $NH_4H_2PO_4$ were replaced with 1 mM KH_2PO_4. For the NsD, 4 mM $Ca(NO_3)_2 \cdot 4H_2O$ and 6 mM KNO_3 were replaced with 4 mM $CaCl_2$ and 6 mM KCl, respectively. For the NsE, maintained full strength Hoagland's nutrient solution. Finally, for the NsF treatment, 4 mM $Ca(NO_3)_2 \cdot 4H_2O$, 6 mM KNO_3 and 1 mM $NH_4H_2PO_4$ were replaced with 7.5 mM $CO(NH_2)_2$, 4 mM $CaCl_2$, 1 mM KH_2PO_4 and 6 mM KCl. In present study, all nutrient solutions were supplied with 5 mg L^{-1} Cd(II) ions and 250 mg L^{-1} GnZVI@DE. In addition, two pots wheat seedling were exposed to Cd-added NsE and Cd-added NsE treated with GnZVI@DE to reveal the underlying mechanism of Cd uptake by wheat mediated by GnZVI@DE amendments. Growth was allowed to continue for another 7 days and then 36 wheat seedlings were collected for further analyses.

Experiment S3: Rhizosphere pH Effect by Nutrients

Compared with NsA, the significant decrease of the rhizosphere pH in the presence of P (NsE) were measured (Figure S5A), which should be attribute to the exudation of carboxylate from wheat roots under P nutrient. In the presence of P, addition of NO_3^-–N in NsC, NH_4^+–N in NsD or urea–N in NsF could significantly affect the rhizosphere pH when were compared to NsB. NO_3^-–N significantly increased the rhizosphere pH from 6.1 to 7.4 (Figure S5A), while NH_4^+–N could significantly decrease the pH value from 6.1 to 3.8. These phenomena were because when wheat absorb NO_3^-–N, the roots generally excrete net excess OH^-. In contrast, excess H^+ were released from wheat roots when the NH_4^+–N was assimilated.[6] Note that when the urea–N was present in NsF, the pH was the highest of all N treatment groups (Figure S5A, NsB–F). This should be associated with the hydrolysis of urea catalyzed by urease which secreted by wheat roots or microorganisms in nutrient solutions.[7]

Experiment S4: Determination of Oxidative Stress–related Indicators

The above–ground tissues of plants, especially leaves, are considered as the most sensitive tissue to heavy metals like Cd.[8] Cd stress can produce excess reactive oxygen species (ROS, mainly include hydrogen peroxide (H_2O_2), hydroxyl radicals ($OH•$) and superoxide radicals ($O_2•^-$)) in plants, which potentially cause oxidative damage to proteins, DNA, and lipids.[9] Malondialdehyde (MDA) content can be typically used as the indicator of lipid peroxidation in plants, which was positively correlated with the Cd accumulation in plant tissues.[10]

In vivo image of ROS. To quantify ROS in vivo, three wheat leaves and roots exposure to Cd growing in NsE with and without GnZVI@DE treatment (compared to that with no Cd or GnZVI@DE) were dyed by the H_2DCFDA.[11] The leaves and roots were incubated in 25 μm H_2DCFDA dye (dissolved in dimethyl sulfoxide (DMSO)) for 30 min under darkness. The samples were then observed by a confocal microscope (Leica TCS SP8 X, Germany). The imaging settings were as

follows: 20× wet objective; 488 nm laser excitation; PMT: 500–600 nm.

MDA content assay. The determination of MDA content in plant leaves was carried out according to the method previously described by Heath with some minor modification.[12] Fresh shoots powders (0.2 g) were quickly homogenized with 4.0 mL of 10.0% (w/v) trichloroacetic acid (TCA), then centrifuging (4℃, 4000 rmp) for 10 min using a freezing centrifuge to obtain extracts. 2.0 mL 0.6% (w/v) thiobarbituric acid (TBA) was added to 2.0 mL of the liquid to be tested and the mixture was reacted in a water bath (100°C) for 15 min, rapidly cooled and filtered. The filtrate was measured using a UV spectrophotometer at λ=532, 600 and 450 nm for absorbance values. Under high temperature and acidic conditions, TBA reacted with MDA in the sample to produce a reddish–brown substance, which was used to assess lipid peroxidation in plant tissues.

Antioxidant enzymes activities

The increase of enzymes (such as SOD, POD and CAT) activities in plants are considered as important indicators for plant to fight against oxidative damage, since SOD catalyzes the reaction of $O_2^{\bullet -}$ to H_2O_2 while CAT and POD promote the conversion of H_2O_2 to H_2O.[9] Thus, the activities of SOD, POD and CAT in shoots were measured to evaluate Cd stress in shoots after GnZVI@DE treatment under different nutrients.

For the SOD activity, it was measured with an assay kit purchased from Nanjing Jiancheng Bioengineering Institute, Nanjing, China

For the POD activity assay, fresh shoots powders (0.1 g) were quickly homogenized in a pre–cooling phosphate buffer solution (0.9 mL) at pH 7.8, then centrifuging (4℃,12000 rmp) for 10 min to obtain crude enzymes extracts. The crude enzymes boiled for 5 min was used as a control, and the reaction system (Phosphate buffer solution:2% H_2O_2:0.05 M Guaiacol solution: crude enzymes solution=2.9 mL:1.0 mL:1.0 mL:0.1 mL) was kept at 37℃ for 15 min immediately after the crude

enzyme added, then quickly transferred to ice and 2.0 ml TCA (20%) was added to terminate the reaction. After filtration, the absorbance was measured using a UV spectrophotometer at λ=470 nm.

For the CAT activity assay, fresh shoots powders (0.1 g) were quickly homogenized in a pre–cooling phosphate buffer solution (0.9 ml) at pH 5.5, then centrifuging (4℃, 12000 rmp) for 10 min to obtain crude enzymes extracts. The crude enzymes were mixed with 30% H_2O_2, and then the mixtures were immediately measured in the wavelength of 240 nm for 2 min each 30 s by a UV spectrophotometer. The CAT activity was assayed by monitoring the degradation of H_2O_2. One unit of CAT is the amount of enzyme that decomposes 1 μmol H_2O_2 per minute.

Experiment S5: Photosynthetic Pigments Content Quantification

The photosynthetic pigments' content was measured following the method described by Wellburn with some minor modification.[13] Briefly, 0.2 g fresh wheat shoots were placed in a mortar and pestle with a small amount of quartz sand and magnesium carbonate powder and 10 mL ethanol (95.0%), ground until the plant tissue was white, after which the ground mixture was filtered into a 25.0 mL brown volumetric flask. The absorbance was measured using a UV spectrophotometer at λ=665 nm, 649 nm and 470 nm respectively, and the chlorophyll a (Chl a), chlorophyll b (Chl b) and carotenoid concentrations (Cx+c) were calculated using the following equations:

$$\text{Chl a} = 13.95 \times A_{665} - 6.88 \times A_{649}$$

$$\text{Chl b} = 24.95 \times A_{649} - 7.32 \times A_{665}$$

$$\text{Cx+c} = (1000 \times A_{470} - 2.05 \times \text{Chl a} - 114.8 \times \text{Chl b})/245$$

Experiment S6: Soluble Protein Content Quantification

The soluble protein content in shoots was measured following the method described by Bradford with some minor modification.[14] Fresh shoots powders (0.1 g) were quickly homogenized in a pre–cooling phosphate buffer solution (0.9 ml) at pH 7.0, then centrifuging (4℃, 4000 rmp) for 10 min to

obtain extracts. After which 2.5 mL Coomassie brilliant blue G–250 staining solution was mixed with 0.5 mL supernatant, left for 5–20 min, and determined at λ=595 nm using a UV spectrophotometer. It was worth noting that the determination of soluble protein should be done within 1 h of reaction period.

Experiment S7: Analysis Methods of Cd and Fe in Wheat Tissues

Extraction of Cd on roots surface was conducted according to the dithionite–citrate–bicarbonate (DCB) method with some slight modifies.[15] Briefly, put the washed fresh roots into a 50 mL centrifuge tubes, then add 40 mL sodium citrate (0.3 M), 5 mL sodium bicarbonate (1 M), finally add 3 g sodium dithionite before putting on an end–to–end rotator at 300 rpm and at room temperature for 3 h. Then the roots were washed three times with DI water, the cleaning solution and the extracting solution were poured into 100 mL volumetric flask. The DCB–Cd in the extracts after pressing through 0.45 μm filters was determined by inductively coupled plasma mass spectrometer (ICPE–9000, Shimadzu Co. Ltd., Japan), respectively.

Washed fresh shoots and roots after extracting Cd adhering to the surface were dried to constant weight (105 ℃ for 1 h and 70℃ for 48 h). The dried wheat samples were crushed and sieved, then digested in a microwave digestion (steps were as following: 120°C (10 min)–150°C (15 min)–190°C (25 min)) with a mixture containing system HNO_3 and H_2O_2 (5:2, v/v), followed by heating at 220°C on a plate digester to drive out the acid. The Cd and Fe in digestion solutions of roots and shoots after filtering and diluting determined by ICPE.[16]

SUPPLEMENTAL RESULTS AND DISCUSSIONS

Result S1: Fe Accumulation in Roots and Shoots with GnZVI@DE Treatment Affected by Nutrients

Compared to NsA, P in NsF significantly reduced Fe accumulation in the roots and shoots by 34.7% and 29.1%, respectively (Figure 1C). This could be explained by the formation of Fe−phosphate

precipitates,[17] which reduced the bioavailable Fe for wheat growth. In the presence of P, different forms of N affect Fe accumulation and translocation differently (Figure 1C and 1B). More specifically, NO_3^-−N in NsC (*vs.* NsB) significantly decreased Fe concentrations by 16.6% in roots and by 20.8% in shoots (Figure 1C). This was likely because NO_3^-−N addition increased the rhizosphere pH (Figure S5A), and caused a differential expression of genes as well as transcriptional regulators to inhibit Fe uptake and transport.[18, 19] By contrast, Fe concentration was significantly increased by 49.7% in roots and by 19.5% in shoots after NH_4^+−N addition in NsD when compared with NsB (Figure 1C), due to NH_4^+−N uptake by wheat made proton efflux with rhizosphere acidification (Figure S5A), increasing the dissolution of Fe(0) core in GnZVI@DE.[6, 17]. Further, the combined NO_3^-−N and NH_4^+−N in NsE (*vs.* NsB) dramatically decreased Fe concentrations in roots and shoots by 27.0% and 23.9%, respectively (Figure 1C). This was likely because combined NO_3^-−N and NH_4^+−N maintained the consistent rhizosphere pH as above discussed (Figure S5A). In addition, urea−N in NsF significantly respectively increased Fe concentrations by 93.6% and 15.0% in roots and shoots when compared to NsB (Figure 1C). This is likely because the dissolved Fe from GnZVI@DE formed a complex with urea−N,[20] which permeated through the cuticular membranes of plant root cells by diffusion, due to its neutrality and low molecular weight.[21]

Meanwhile, the Fe $TF_{root–shoot}$ values of wheat under various nutrient conditions were calculated, as shown in Figure 1B. With the addition of GnZVI@DE amendment, the Fe $TF_{root–shoot}$ in wheat was significantly enhanced (Table S1), whereas the Cd $TF_{root–shoot}$ was decreased, which was likely because Fe and Cd translocation in plants could be mediated by the same transporter genes.[18, 22, 23] Compare to NsA, P in NsE slightly increased Fe $TF_{root–shoot}$ by 8.5% (Figure 1B), which meant that P slightly inhibited Fe translocation from roots to shoots in wheat. The NH_4^+−N (NsD *vs.* NsB) and urea−N (NsF *vs.* NsB) addition significantly decreased Fe $TF_{root–shoot}$ by 46.2% and 55.7%, respectively (Figure 1B).

This was attributed to strengthened Fe binding with the cell wall of roots, leading to less bioavailable Fe.[5] Notably, Fe $TF_{root–shoot}$ increased with a decrease in Cd $TF_{root–shoot}$ in all N and P nutrient solutions, except the single NO_3^-−N in NsC (Figure 1B).

Result S2: Chemical Reactions Between GnZVI@DE and Cd(II) Ions Affected by Nutrients

Through batch experiments, we studied the interactions between different nutrients (P, NO_3^-–N, NH_4^+–N or urea–N), Cd(II) ions and GnZVI@DE. First, 250 mg L^{-1} GnZVI@DE was suspended in DI water before being ultrasonicated. Then, 2.5–40 mg L^{-1} Cd(II) ions solution was prepared with 1 mM NaCl solutions, containing with 1 mM P, 14 mM NO_3^-, 1 mM NH_4^+ or 7.5 mM urea nutrients (consistent with four component concentrations in full–strength Hoagland's nutrient solution as described in Experiment S2). The pH of three aliquots of the suspension was adjusted to 6.0 with 1 mM NaOH/HCl solutions to simulate pH of natural soil environment in rhizosphere. Three parallel samples were transferred to 50 mL centrifuge tubes before putting on an end–to–end rotator at 300 rpm for 3 h.[1] The suspension was centrifuged using an ultrahigh–speed freezing centrifuge (10,000 rpm, 20 min) before passing through a 0.45 μm membrane filter. Then the concentrations of Cd in the filtrate were measured by ICP.[3]

The Cd removal capacity of GnZVI@DE was quantified in the presence of P, NO_3^-, NH_4^+ or urea (Figure S3). With the increase of Cd concentration from 2.5 to 40.0 mg L^{-1}, the Cd removal capacity of amendment without nutrients (CK) from water was increased from 10.0 to 75.7 mg g^{-1}, which could be ascribed to more adsorption and reduction at higher Cd concentrations.[3, 17] In the presence of P, the removal capacity was significantly enhanced by 8.1% and 47.9% at 20.0 and 40.0 mg L^{-1} of Cd level. The precipitation of cadmium phosphates under high Cd concentration is presumed to be a possibility for this phenomenon.[24-26] Note that NO_3^- showed potent inhibition in the Cd removal of GnZVI@DE amendment, which might be attributed to the inhibited corrosion of Fe(0) by NO_3^-.[27] Also, NH_4^+

significantly inhibited Cd removal at high level of Cd (Figure S3). NH_4^+ could adsorb onto nZVI through electrostatic attraction, cation exchange, and adsorption.[28] Thus, we reasonably speculated that NH_4^+ compete with Cd(II) ions for similar adsorption sites on GnZVI@DE, resulting in less Cd(II) ions adsorption and more exchangeable Cd(II) ions in solution. In addition, urea enhanced Cd removal by GnZVI@DE with increasing Cd concentration, especially increase by 24.4% compared to CK at 40.0 mg L^{-1} Cd concentration. This was likely attributed to the increased dispersity of GnZVI@DE (Figure 3C), resulting from the generated steric hindrance on GnZVI@DE by urea for favorite Cd removal by GnZVI@DE amendments.

Result S3: Zeta Potentials of GnZVI@DE

To better understand the Cd removal mechanism by GnZVI@DE with the coexistence of different P, NO_3^-, NH_4^+ or urea nutrients, the surface properties of GnZVI@DE–Cd were investigated under various conditions. As shown in Figure 3A, surface zeta potentials of GnZVI@DE (CK) were negatively charged (−35.6 mV) in 1 mM NaCl solution at pH 6, which was similar to previous researches.[3, 29] Further, the surface charges of GnZVI@DE particles were pronouncedly reduced by NO_3^- or NH_4^+ adsorption. Thus, the repulsion forces between GnZVI@DE particles decreased, associated with increased particle size due to the suppressed electrostatic double layer based on Derjaguin–Landau–Vervey–Overbeek (DLVO) theory.[17, 30] This contributed to less Cd(II) adsorption compared to the GnZVI@DE nanoparticles alone (CK, without the presence of N and P) (Figure S3). In opposite, the P or urea appearance enhanced negative surface charges of GnZVI@DE, leading to the decreased particle size (Figure 3A, P or Urea *vs.* CK and Figure 3B, P & Cd or Urea & Cd *vs.* CK & Cd). Therefore, the stability of GnZVI@DE particles was better in P or urea than that in NO_3^- or NH_4^+ solutions (Figure 3C, P or Urea *vs.* NO_3^- or NH_4^+ and Figure 3D, P & Cd or Urea & Cd *vs.* NO_3^- & Cd or NH_4^+ & Cd). This appears that P or urea increased Cd(II) ions adsorption of GnZVI@DE

particles (Figure S3), which was consistent with reports that the smaller particles with larger surface area have more adsorption sites for more Cd(II) ions adsorption.[31, 32]

Result S4: Effects of Nutrients on Soluble protein and Photosynthetic Pigment Content in Shoots under GnZVI@DE Treatment

Normally, plants produce specific soluble proteins that bind to Cd(II) ions to mitigate their detrimental effects.[3] As shown in Figure S6, GnZVI@DE amendment decreased the level of Cd accumulation, consequently reducing the soluble proteins in Cd-exposed wheat leaves by 29.1%. In addition, the accumulation of Cd(II) in plants destroyed the chloroplast structure and accelerated the decomposition of photosynthetic pigments, ultimately reducing their concentration.[33] After treatment with GnZVI@DE alone, the photosynthetic pigments of wheat leaves were enhanced by 35.3% (Figure S6) due to lower Cd accumulation, compared with those leaves not subjected to the amendment (Table S1).

Especially, P addition in NsE significantly decreased the soluble proteins in the shoots compared with NsA (Figure 5E), due to the further lower Cd accumulation. In contrast, NO_3^-−N, NH_4^+−N, or the combination of NO_3^-−N and NH_4^+−N significantly increased the soluble protein content (Figure 5E, NsC–E *vs.* NsB), because increasing N concentrations facilitate protein synthesis. It should be noted that the soluble protein content was higher in shoots exposed to urea−N in NsF than to NO_3^-−N in NsC or NO_3^-−N and NH_4^+−N in NsE (Figure 5E). This was likely due to the fact that urea can be hydrolyzed to HCO_3^- and NH_3 (or NH_4^+) by urease in plant cells.[34] As shown in Figure 5F, P significantly increased the photosynthetic pigment content (NsE *vs.* NsA). Similarly, this parameter was higher in shoots grown under N nutrients (NsC–F) than without them in NsB (Figure 5F). This indicated that the synergetic effect of N deficiency and Cd(II) ions inhibited the production of photosynthetic pigments in the shoots.[35] In particular, the photosynthetic pigment content of shoots

grown in soil treated with a combination of urea−N and P was 3.6 mg g^{-1}, which was considerably higher than that observed in shoots grown under other N nutrient solutions (Figure 5F). This finding is consistent with the relatively lower Cd accumulation observed in shoots grown under urea−N and P nutrients (Figure 1A, NsF).

REFERENCES:

(1) Sun, Z.; Zheng, S.; Ayoko, G. A.; Frost, R. L.; Xi, Y. Degradation of Simazine from Aqueous Solutions by Diatomite-Supported Nanosized Zero-Valent Iron Composite Materials. *J. Hazard. Mater.* **2013**, *263* (Pt 2), 768-77.

(2) Ye, Z.; Xu, N.; Li, D.; Qian, J.; Du, C.; Chen, M. Vitamin C Mediates the Activation of Green Tea Extract to Modify Nanozero-Valent Iron Composites: Enhanced Transport in Heterogeneous Porous Media and the Removal of Hexavalent Chromium. *J. Hazard. Mater.* **2021**, *411*, 125042.

(3) Zhu, F.; Li, L.; Ren, W.; Deng, X.; Liu, T. Effect of pH, Temperature, Humic Acid and Coexisting Anions on Reduction of Cr(VI) in the Soil Leachate by nZVI/Ni Bimetal Material. *Environ. Pollut.* 2017, *227*, 444-450.

(4) Du, C.; Xu, N.; Yao, Z.; Bai, X.; Gao, Y.; Peng, L.; Gu, B.; Zhao, J. Mechanistic Insights into Sulfate and Phosphate-Mediated Hexavalent Chromium Removal by Tea Polyphenols Wrapped Nano-Zero-Valent Iron. *Sci. Total Environ.* **2022**, *850*, 157996..

(5) Cheng, Y.; Bao, Y.; Chen, X.; Yao, Q.; Wang, C.; Chai, S.; Zeng, J.; Fan, X.; Kang, H.; Sha, L.; Zhang, H.; Zhou, Y.; Wang, Y. Different Nitrogen Forms Differentially Affect Cd Uptake and Accumulation in Dwarf Polish Wheat (Triticum Polonicum L.) Seedlings. *J. Hazard. Mater.* **2020**, *400*, 123209.

(6) Lu, H. L.; Nkoh, J. N.; Abdulaha-Al Baquy, M.; Dong, G.; Li, J. Y.; Xu, R. K. Plants Alter Surface Charge and Functional Groups of Their Roots to Adapt to Acidic Soil Conditions. *Environ. Pollut.* **2020**, *267*, 115590.

(7) Sigurdarson, J. J.; Svane, S.; Karring, H. The Molecular Processes of Urea Hydrolysis in Relation to Ammonia Emissions from Agriculture. *Rev. Environ. Sci. Biotechnol.* **2018**, *17* (2), 241-258.

(8) Mir, I. R.; Rather, B. A.; Masood, A.; Anjum, N. A.; Khan, N. A. Nitrogen Sources Mitigate Cadmium Phytotoxicity Differentially by Modulating Cellular Buffers, N-Assimilation, Non-Protein Thiols, and Phytochelatins in Mustard (Brassica Juncea L.). *J. Soil Sci. Plant Nutr.* **2022**, *22* (3), 3847-3867.

(9) Gong, X.; Huang, D.; Liu, Y.; Zeng, G.; Wang, R.; Wan, J.; Zhang, C.; Cheng, M.; Qin, X.; Xue, W. Stabilized Nanoscale Zerovalent Iron Mediated Cadmium Accumulation and Oxidative Damage of Boehmeria Nivea (L.) Gaudich Cultivated in Cadmium Contaminated Sediments. *Environ. Sci. Technol.* **2017**, *51* (19), 11308-11316.

(10) Yang, L. P.; Zhu, J.; Wang, P.; Zeng, J.; Tan, R.; Yang, Y. Z.; Liu, Z. M. Effect of Cd on Growth, Physiological Response, Cd Subcellular Distribution and Chemical Forms of Koelreuteria Paniculata. *Ecotoxicol. Environ. Saf.* **2018**, *160*, 10-18.

(11) Liu, Y.; Yue, L.; Wang, C.; Zhu, X.; Wang, Z.; Xing, B. Photosynthetic Response Mechanisms in Typical C3 and C4 Plants Upon La_2O_3 Nanoparticle Exposure. *Environ. Sci. Nano* **2020**, *7* (1), 81-92.

(12) Heath, R. L.; Packer, L. Photoperoxidation in Isolated Chloroplasts .I. Kinetics and Stoichiometry of Fatty Acid Peroxidation. *Arch. Biochem. Biophys.* **1968**, *125* (1), 189-198.
(13) Wellburn, A. R. The Spectral Determination of Chlorophyll a and b, as Well as Total Carotenoids, Using Various Solvents with Spectrophotometers of Different Resolution. *J. Plant Physiol.* **1994**, *144* (3), 307-313.
(14) Bradford, M. M. A Rapid and Sensitive Method for the Quantitation of Microgram Quantities of Protein Utilizing the Principle of Protein-Dye Binding. *Anal. Biochem.* **1976**, *72*, 248-54.
(15) Gu, S.; Lian, F.; Han, Y.; Taherymoosavi, S.; Mitchell, D.; Joseph, S.; Wang, Z.; Xing, B. Nano-Biochar Modulates the Formation of Iron Plaque through Facilitating Iron-Involved Redox Reactions on Aquatic Plant Root Surfaces. *Environ. Sci. Nano* **2022**, *9* (6), 1974-1985.
(16) Wei, W.; Peng, H.; Xie, Y.; Wang, X.; Huang, R.; Chen, H.; Ji, X. The Role of Silicon in Cadmium Alleviation by Rice Root Cell Wall Retention and Vacuole Compartmentalization under Different Durations of Cd Exposure. *Ecotoxicol. Environ. Saf.* **2021**, *226*, 112810.
(17) Yao, Z.; Wang, D.; Xu, N.; Du, C.; Feng, Y.; Qi, Y. Phosphate and Humic Acid Inhibit Corrosion of Green-Synthesized Nano-Iron Particles to Remove Cr(VI) and Facilitate Their Cotransport. *Chem. Eng. J.* **2022**, *450*, *136415*.
(18) Sun, W. J.; Zhang, J. C.; Ji, X. L.; Feng, Z. Q.; Wang, X.; Huang, W. J.; You, C. X.; Wang, X. F.; Hao, Y. J. Low Nitrate Alleviates Iron Deficiency by Regulating Iron Homeostasis in Apple. *Plant Cell Environ.* **2021**, *44* (6), 1869-1884.
(19) Ye, J. Y.; Zhou, M.; Zhu, Q. Y.; Zhu, Y. X.; Du, W. X.; Liu, X. X.; Jin, C. W. Inhibition of Shoot-Expressed NRT1.1 Improves Reutilization of Apoplastic Iron under Iron-Deficient Conditions. *Plant J.* **2022**, *112* (2), 549-564.
(20) Asuha, S.; Zhao, S.; Jin, X. H.; Hai, M. M.; Bao, H. P. Effects of Synthetic Routes of Fe–Urea Complex on the Synthesis of γ-Fe_2O_3 Nanopowder. *Appl. Surf. Sci.* **2009**, *255* (21), 8897-8901.
(21) Wang, W. H.; Köhler, B.; Cao, F. Q.; Liu, L. H. Molecular and Physiological Aspects of Urea Transport in Higher Plants. *Plant Sci.* **2008**, *175* (4), 467-477.
(22) Guerinot, M. L. The ZIP Family of Metal Transporters. *Biochim. Biophys. Acta* **2000**, *1465* (1-2), 190-198.
(23) He, X. L.; Fan, S. K.; Zhu, J.; Guan, M. Y.; Liu, X. X.; Zhang, Y. S.; Jin, C. W. Iron Supply Prevents Cd Uptake in Arabidopsis by Inhibiting IRT1 Expression and Favoring Competition between Fe and Cd Uptake. *Plant Soil* **2017**, *416* (1-2), 453-462.
(24) Tiberg, C.; Gustafsson, J. P. Phosphate Effects on Cadmium(Ii) Sorption to Ferrihydrite. *J. Colloid Interface Sci.* **2016**, *471*, 103-111.
(25) Seshadri, B.; Bolan, N. S.; Choppala, G.; Kunhikrishnan, A.; Sanderson, P.; Wang, H.; Currie, L. D.; Tsang, D. C. W.; Ok, Y. S.; Kim, G. Potential Value of Phosphate Compounds in Enhancing Immobilization and Reducing Bioavailability of Mixed Heavy Metal Contaminants in Shooting Range Soil. *Chemosphere* **2017**, *184*, 197-206.
(26) Huang, K.; Hu, C.; Tan, Q.; Yu, M.; Shabala, S.; Yang, L.; Sun, X. Highly Efficient Removal of Cadmium from Aqueous Solution by Ammonium Polyphosphate-Modified Biochar. *Chemosphere* **2022**, *305*, 135471.
(27) Wei, A.; Ma, J.; Chen, J.; Zhang, Y.; Song, J.; Yu, X. Enhanced Nitrate Removal and High Selectivity Towards Dinitrogen for Groundwater Remediation Using Biochar-Supported Nano Zero-Valent Iron. *Chem. Eng. J.* **2018**, *353*, 595-605.
(28) Eljamal, O.; Eljamal, R.; Maamoun, I.; Khalil, A. M. E.; Shubair, T.; Falyouna, O.; Sugihara, Y. Efficient Treatment of Ammonia-Nitrogen Contaminated Waters by Nano Zero-Valent Iron/Zeolite

Composite. *Chemosphere* **2022**, *287* (Pt 1), 131990.
(29) Yang, H.; Ye, Z.; Feng, F.; Xu, N.; Yang, J.; Yao, Z.; Li, Z.; Chen, J. Green-Synthesized Nanosize Mont-Supported Fe^0 via Tea Extract for Enhanced Transport and in Situ Remediation of Pb(II) in Soil. *J. Soils Sediments* **2021**, *21* (7), 2540-2550.
(30) Zhang, M.; He, F.; Zhao, D.; Hao, X. Transport of Stabilized Iron Nanoparticles in Porous Media: Effects of Surface and Solution Chemistry and Role of Adsorption. *J. Hazard. Mater.* **2017**, *322* (Pt A), 284-291.
(31) He, C.; Xie, F. Adsorption Behavior of Manganese Dioxide Towards Heavy Metal Ions: Surface Zeta Potential Effect. *Water Air Soil Pollut.* **2018**, *229*, 77.
(32) Wang, H.; Liang, J.; Huo, P.; Zhang, L.; Fan, X.; Sun, S. Understanding the Cadmium Passivation and Nitrogen Mineralization of Aminated Lignin in Soil. *Sci. Total Environ.* **2023**, *873*, 162334.
(33) Ren, T.; Chen, N.; Wan Mahari, W. A.; Xu, C.; Feng, H.; Ji, X.; Yin, Q.; Chen, P.; Zhu, S.; Liu, H.; Liu, G.; Li, L.; Lam, S. S. Biochar for Cadmium Pollution Mitigation and Stress Resistance in Tobacco Growth. *Environ. Res.* **2021**, *192*, 110273.
(34) Ruan, Z.; Giordano, M. The Use of NH_4^+ Rather Than NO_3^- Affects Cell Stoichiometry, C Allocation, Photosynthesis and Growth in the Cyanobacterium Synechococcus Sp. UTEX LB 2380, Only When Energy Is Limiting. *Plant Cell Environ.* **2017**, *40* (2), 227-236.
(35) Li, L.; Wang, Y. Independent and Combined Influence of Drought Stress and Nitrogen Deficiency on Physiological and Proteomic Changes of Barley Leaves. *Environ. Exp. Bot.* **2023**, *210*.

ADDITIONAL TABLE

Table S1 Cd and Fe accumulation in the shoots and roots of wheat seedlings and relevant metal translocation factors from roots to shoots exposure Cd with and without GnZVI@DE treatment.

Metals accumulation and Translocation	Without Cd and GnZVI@DE (No)	250 mg L^{-1} GnZVI@DE	5 mg L^{-1} Cd	5 mg L^{-1} Cd with 250 mg L^{-1} GnZVI@DE
Cd content in roots (mg kg^{-1})	0	0	537.5±25.8	329.2±7.8
Cd content in shoots (mg kg^{-1})	0	0	63.2±7.0	37.5±0.9
Cd translocation factor	0	0	14.0%	11.0%
Fe content in wheat roots (mg kg^{-1})	276.5625±8.1	331.25±19.8	167.1875±9.2	229.7±9.2
Fe content in wheat shoots (mg kg^{-1})	146.375±8.51	177.8125±11.1	45.1±4.8	71.7±2.1
Fe translocation factor	48.3%	53.7%	22.2%	31.2%

ADDITIONAL FIGURES

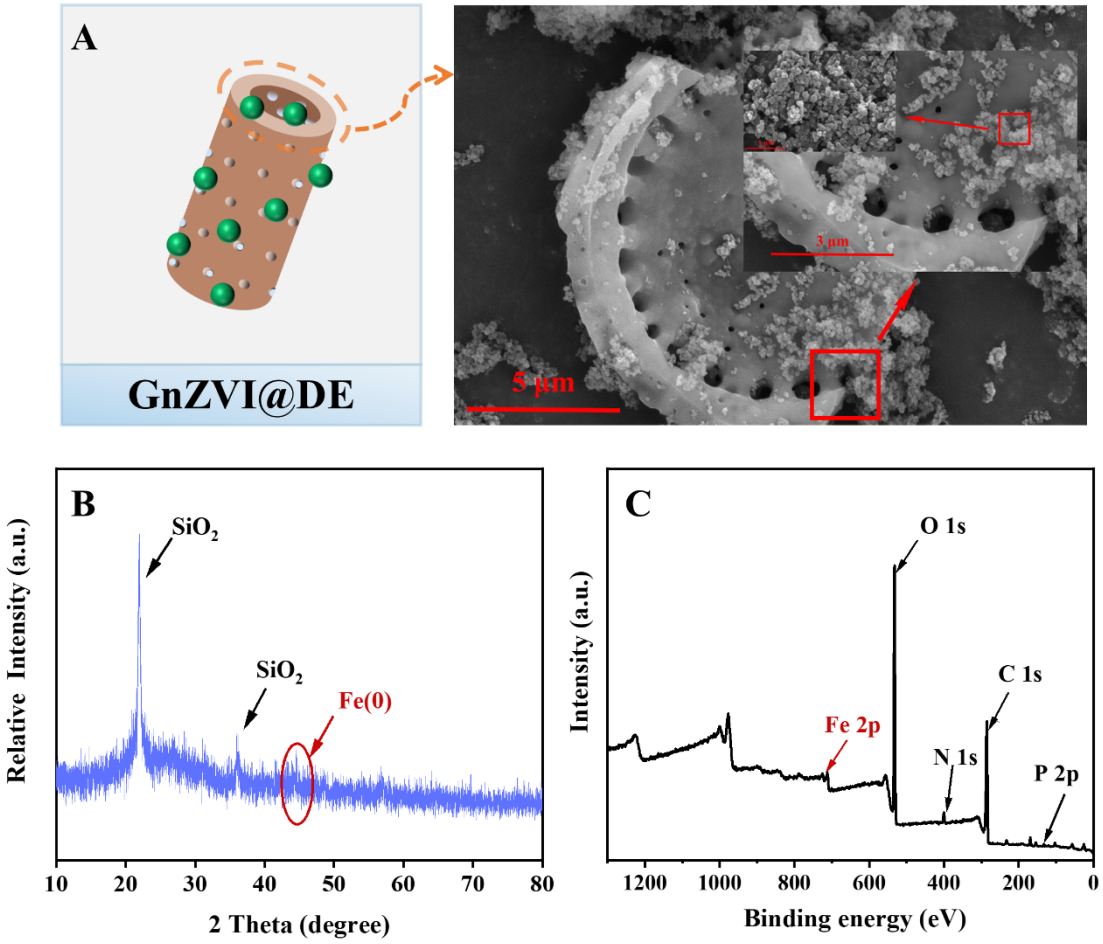

Figure S1 SEM image (A), XRD patterns (B), and XPS full scan spectrum (C) of GnZVI@DE.

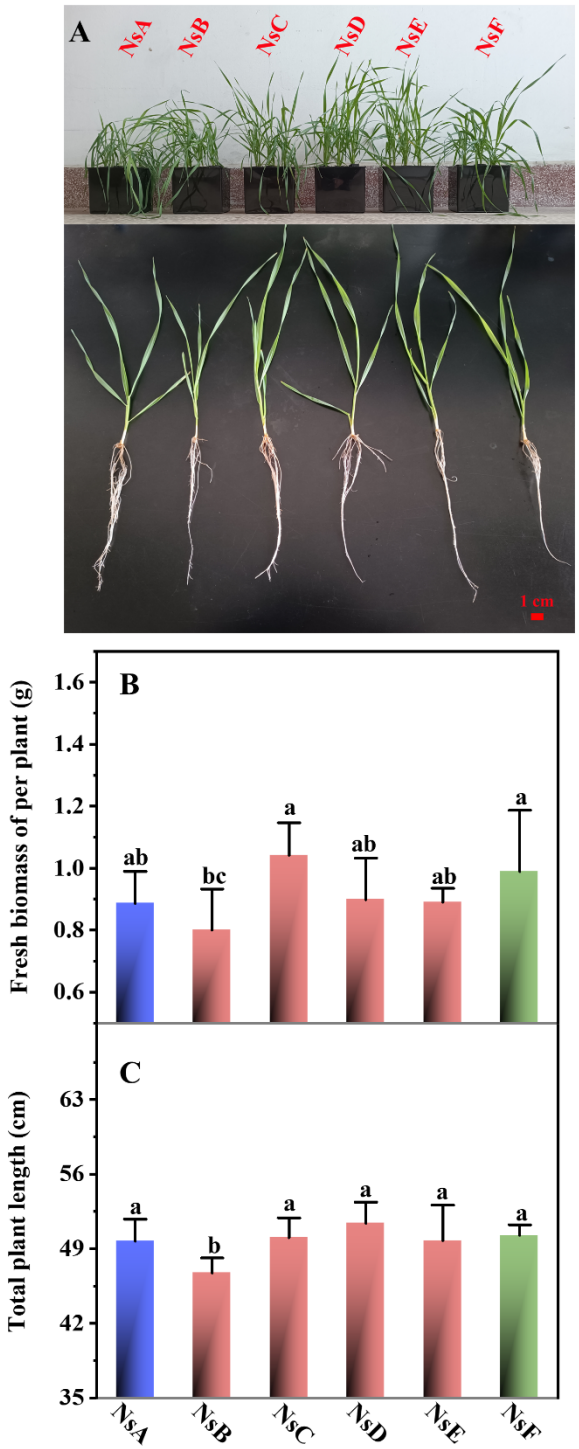

Figure S2 Picture of wheat seedlings (A), changes of fresh biomass (B), and total plant length of wheat (C) grown for 7 days in different P and N nutrient solutions [containing 5 mg L^{-1} Cd(II) and 250 mg L^{-1} GnZVI@DE]. (NsA, NO_3^-–N & NH_4^+–N; NsB, P; NsC, NO_3^-–N & P; NsD, NH_4^+–N & P; NsE, NO_3^-–N & NH_4^+–N & P; NsF, urea−N & P). Different letters above the error bars indicate significant differences among treatments ($p < 0.05$).

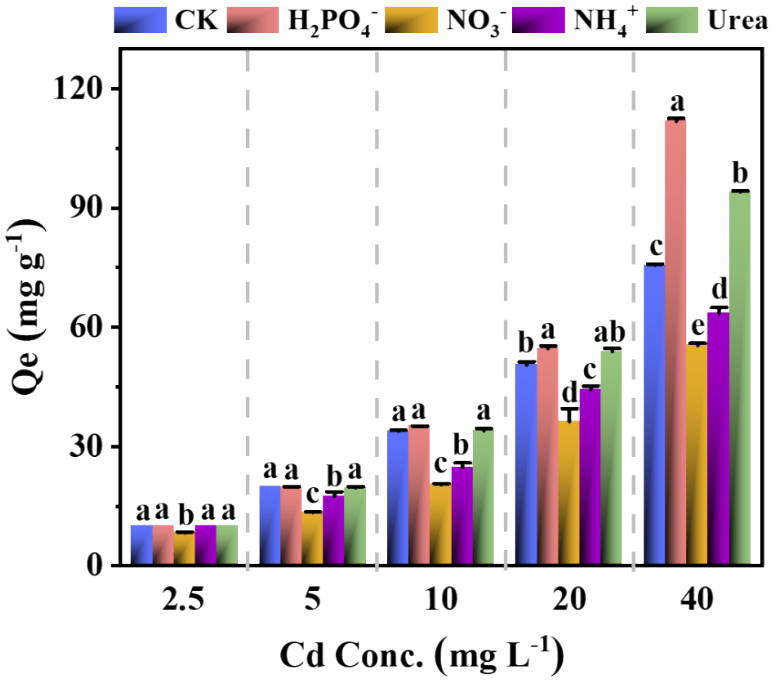

Figure S3 Effect of P, NO_3^-, NH_4^+ and urea on Cd(II) removal by 250 mg L^{-1} GnZVI@DE (CK) in 1mM NaCl electrolyte solution at pH 6.0. Different letters above the error bars indicate significant differences among the treatments ($p < 0.05$).

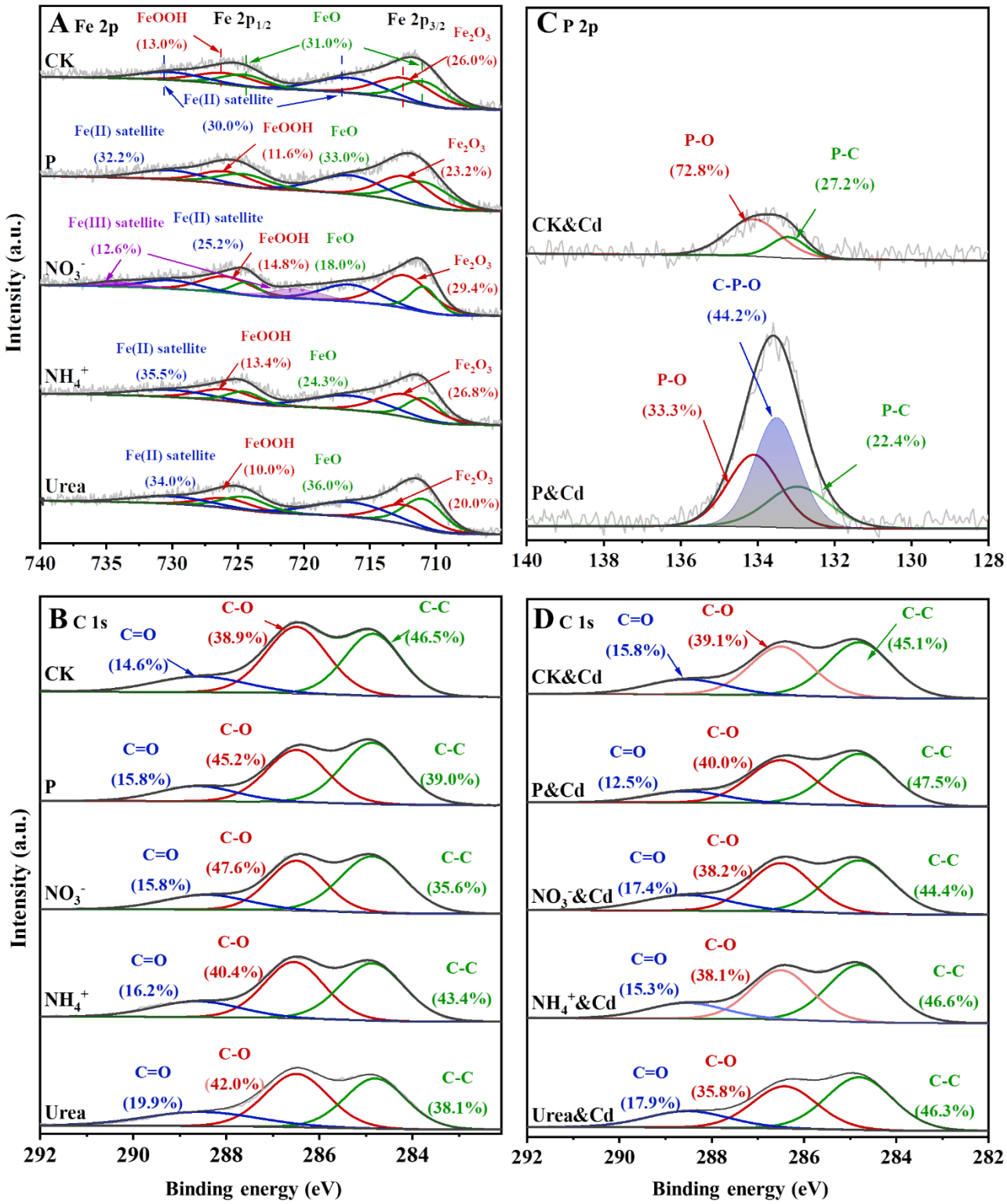

Figure S4 XPS spectra of Fe 2p (A), C 1s (B, D) and P 2p (C) of GnZVI@DE (CK) before (A, B) and after (C, D) reacting with Cd(II) ions in the presence of P, NO_3^-, NH_4^+ and urea at pH 6.0.

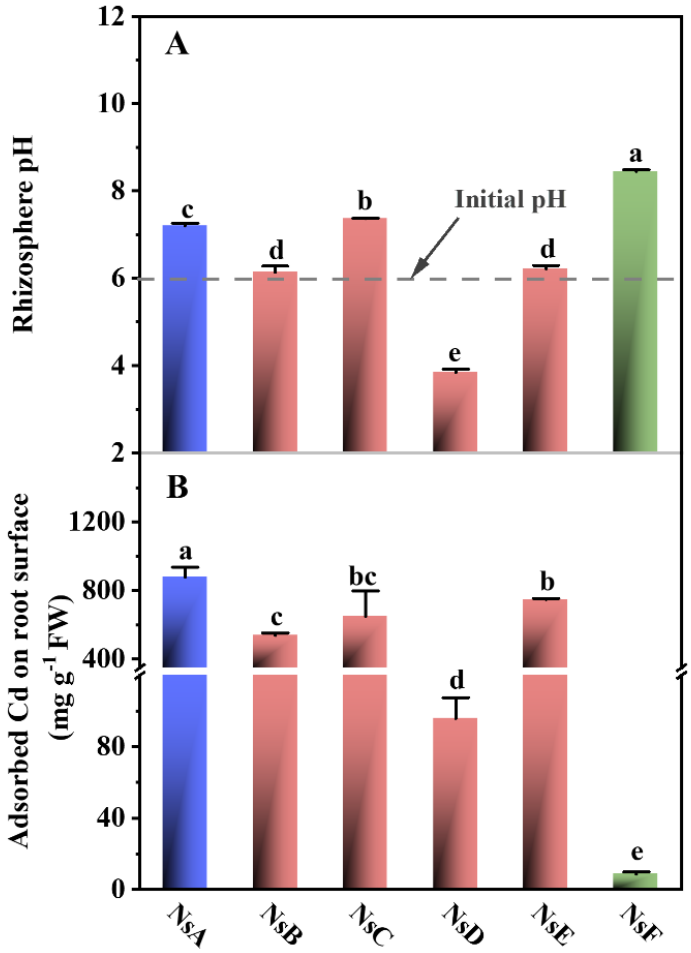

Figure S5 Changes of rhizosphere pH (A), and absorbed Cd on the root surface of wheat (B) grown for 7 days in different P and N nutrient solutions [containing 5 mg L^{-1} Cd(II) and 250 mg L^{-1} GnZVI@DE]. (NsA, NO_3^-–N & NH_4^+–N; NsB, P; NsC, NO_3^-–N & P; NsD, NH_4^+–N & P; NsE, NO_3^-–N & NH_4^+–N & P; NsF, urea–N & P). Different letters above the error bars indicate significant differences among treatments ($p < 0.05$).

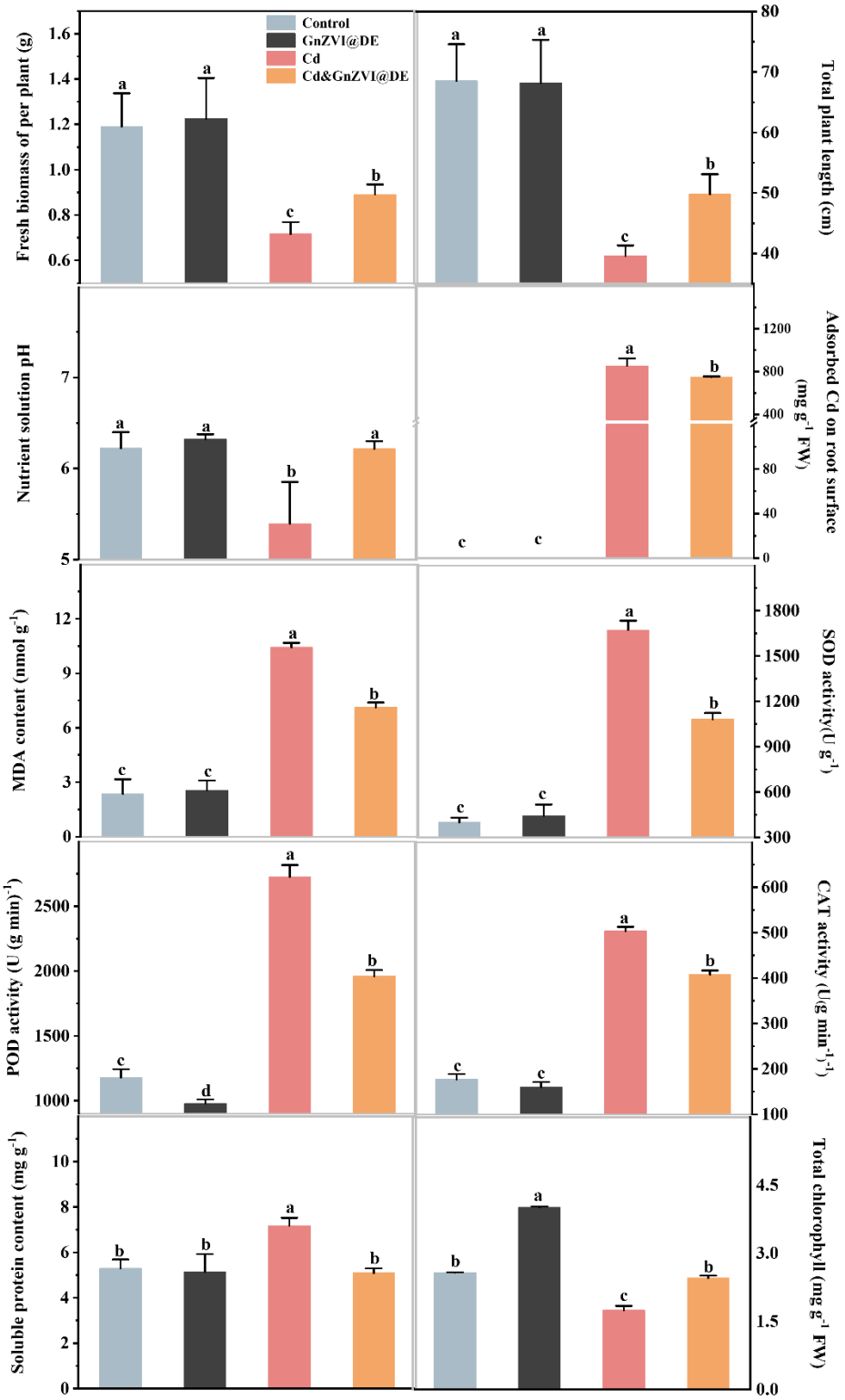

Figure S6 Changes of physiological parameters of wheats growing under various conditions of NsE without Cd and GnZVI@DE (Control), NsE with GnZVI@DE (250 mg L^{-1}), NsE with Cd (5 mg L^{-1}), and NsE with 5 mg L^{-1} Cd treated with 250 mg L^{-1} GnZVI@DE amendments. Different letters above the error bars indicate significant differences among treatments ($p < 0.05$).